

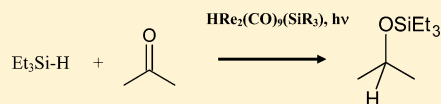
Catalytic Hydrosilylation of Carbonyls via $\text{Re}(\text{CO})_5\text{Cl}$ Photolysis

Chun Keong Toh, Yin Ngai Sum, Wai Kit Fong, Siau Gek Ang, and Wai Yip Fan*

Department of Chemistry, National University of Singapore, 3 Science Drive 3, Singapore 117543.

ABSTRACT: The hydrosilylation reaction between silanes and various carbonyl substrates such as aldehyde, ketone, ester, and carbonate has been catalyzed by $\text{Re}(\text{CO})_5\text{Cl}$ UV photolysis. Kinetic studies have shown that the reaction is favored for the least sterically hindered silanes with aldehydes followed by aliphatic ketones.

The IR spectrum of the rhenium carbonyl dimer $\text{HRe}_2(\text{CO})_9(\text{SiR}_3)$ has been recorded in the reaction mixture. This complex is believed to be the resting state of the active catalyst $\text{Re}(\text{CO})_4\text{SiR}_3$, which could be released upon photactivation. A catalytic mechanism involving this species has been proposed and shown to be thermodynamically feasible using computational studies. In addition, the relative hydrosilylation rates among the various carbonyl substrates can be explained using the same mechanism.



INTRODUCTION

The reaction of silanes with a wide range of carbonyl compounds remains important in the generation of useful protecting groups for organic synthesis. For example, hydrosilylation across the $\text{C}=\text{O}$ bond of aldehydes and ketones produces protected alcohols in a single step.¹ In the presence of a catalyst, these reactions could be carried out under mild conditions, in contrast to using harsh reducing agents such as lithium aluminum hydride. Hydrosilylation catalysis has been reported for various transition-metal complexes containing iron,^{2,3} tungsten,⁴ molybdenum,⁵ manganese,^{6,7} rhenium,^{1,8} rhodium,⁹ silver,¹⁰ and most recently ruthenium.¹¹ Recent work was also done on the mechanistic studies of hydrosilylation using oxo-rhenium complexes.^{12,13}

While Berke et al.⁸ have reported the use of different rhenium(I) catalysts for the hydrosilylation of aldehydes and ketones, one of the more interesting processes is the $\text{CpFe}(\text{CO})_2\text{Me}$ -catalyzed reaction between silanes and dimethylformamide (DMF) reported by Pannell et al.¹⁴ As shown in Scheme 1, hydrosilylation across the $\text{C}=\text{O}$ bond of DMF first afforded a silyl ether which further reacted with another molecule of silane to give siloxane and trimethylamine as final products. Cutler et al.¹⁵ have used the manganese complex $(\text{CO})_5\text{Mn}(\text{C}(\text{O})\text{CH}_3)$ to reduce the much less reactive ester to ether via a silyl acetal intermediate. Silyl esters are another important class of silicon-containing compounds, as they find wide use in the production of polymeric materials.¹⁶ Mizuno et al.¹⁶ reported that a range of ruthenium catalysts enables the conversion of carboxylic acids to silyl esters to take place. Furthermore, Yamamoto's group showed that a boron catalyst, $\text{B}(\text{C}_6\text{F}_5)_3$, reduces carboxylic acids further to the corresponding alkanes as depicted in Scheme 1.¹⁷ However, most of the reported carbonyl hydrosilylation catalysts require careful handling, as they are relatively unstable under ambient conditions.

Although the commercially available rhenium(I) complexes $\text{Re}(\text{CO})_5\text{X}$ ($\text{X} = \text{Br}, \text{Cl}, \text{Re}(\text{CO})_5$) have been reported to activate Si-H bonds, their activity toward carbonyl hydrosilylation has not been explored fully.¹⁸ It was previously reported¹⁹ that the air- and moisture-stable $\text{Re}(\text{CO})_5\text{Cl}$

dissociates a CO ligand readily upon photolysis (quantum yield of 0.06 to 0.44 from 366 nm to 313 nm). In light of efforts to utilize energy from light rather than from fossil fuel sources, much work would have to be carried out to further explore light-driven catalytic processes. As it is also desirable for the catalysts to be air and moisture stable and easy to handle, we have photoactivated $\text{Re}(\text{CO})_5\text{Cl}$ and other rhenium carbonyls in order to carry out hydrosilylation reactions on a variety of carbonyl substrates at room temperature. The objectives of the work are to determine the relative efficiency of the catalysts toward different carbonyls, identify possible key catalytic intermediates, and explore the mechanism of hydrosilylation using a combination of IR and NMR spectroscopy as well as computational studies.

RESULTS AND DISCUSSION

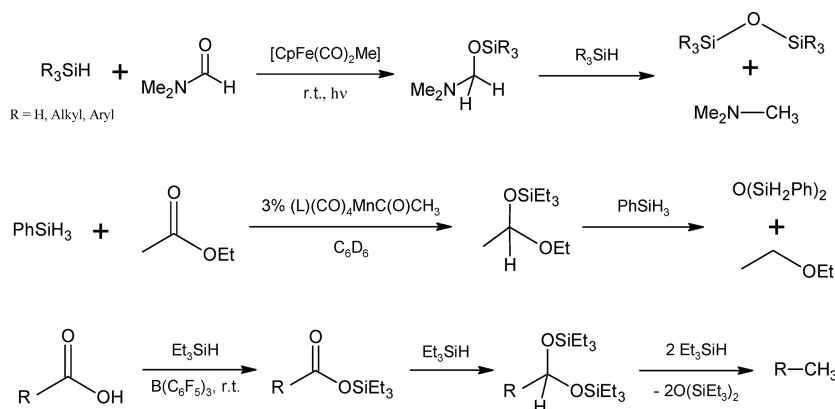
Hydrosilylation of Aldehydes and Ketones. Preliminary experiments have been carried out to assess the efficiency of $\text{Re}(\text{CO})_5\text{Cl}$ UV photolysis toward carbonyl hydrosilylation using Et_3SiH and acetone as substrates (Table 1, entry 1). The quantum yields for $\text{Re}(\text{CO})_5\text{Cl}$ dissociation at 313 and 366 nm have been determined to be 0.44 and 0.06, respectively.¹⁹ The light source used in our work is broad band, ranging from 300 to 800 nm. Since $\text{Re}(\text{CO})_5\text{Cl}$ absorbs in the 300–350 nm region, the quantum yield would also be expected to be similar to the range quoted. ^1H NMR analysis of the mixture after 4 h of photolysis showed isopropoxytriethylsilane, $\text{Et}_3\text{SiOCH}(\text{CH}_3)_2$ (**1a**), as the sole product (Figure 1), with a turnover number (TON) determined to be 70–80 with respect to $\text{Re}(\text{CO})_5\text{Cl}$ (1% mol loading).

The reaction appears to proceed most efficiently if an excess of silane is used to achieve full conversion of acetone to the product. A silane:carbonyl ratio of 3:1 has been used for further comparison with other carbonyl substrates. However, the silyl ether **1a** does not undergo further reaction with excess silane. Such is also the case in the $\text{Re}(\text{CO})_5\text{Cl}$ -catalyzed reactions of Et_3SiH with other carbonyl substrates (Table 1, entries 2–6).

Received: December 20, 2011

Published: May 16, 2012

Scheme 1. Catalytic Hydrosilylation of Carbonyl Compounds

Table 1. Reactions of Et₃SiH with Various Aldehydes and Ketones

Entry	Substrate	Catalyst used	Product ^(a)	TOF ^(b) (hr ⁻¹)
1		Re(CO) ₅ Cl		18
2		Re(CO) ₅ Cl		20
3		Re(CO) ₅ Cl		20
4		Re(CO) ₅ Cl		21
5		Re(CO) ₅ Cl		23
6		Re(CO) ₅ Cl		11
7		Re(CO) ₅ Cl		4
8		Re ₂ (CO) ₁₀	(1a)	15
9		Re ₂ (CO) ₁₀	(1b)	18
10		HRe(CO) ₅	(1a)	3
11		HRe(CO) ₅	(1b)	5

^aProduct was obtained after 4 hrs of photolysis in vacuo, with 1% mol loading of catalyst. Ratio of silane to carbonyl substrate is 3:1. ^bTOF = TON/time was calculated based on 4hrs of photolysis in vacuo.

Further control experiments have been carried out. When the mixture was heated from 30 to 120 °C in the absence of light, the yield of the resultant silyl ether was less than 10%. No hydrosilylation product was observed when the mixture was photolyzed in air or upon removal of the rhenium catalyst. In the presence of PPh₃ (about 3 equiv of Re(CO)₅Cl), the Re(CO)₅Cl photocatalysis was severely inhibited with a product yield of less than 5%. An FTIR analysis of the reaction mixture after 4 h of reaction revealed the presence of Re(CO)₄(PPh₃)Cl (2018, 2002, and 1946 cm⁻¹).²⁰

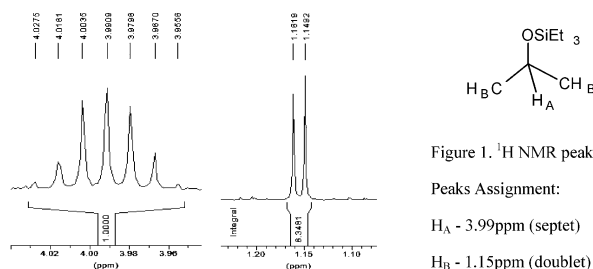


Figure 1. ¹H NMR peaks of 1a. Peak assignment: H_A, 3.99 ppm (septet); H_B, 1.15 ppm (doublet).

Re₂(CO)₁₀ has been found to be an effective catalyst as well (Table 1, entries 8 and 9) with a TON ratio similar to that of Re(CO)₅Cl. However, hydrosilylation proceeded only sluggishly when HRe(CO)₅ was used (Table 1, entries 10 and 11). In comparison to previously reported catalysts⁷ such as [Re(CH₃CN)₃Br₂(NO)] (TON = 99 for aldehydes/ketones), a similar efficiency has been observed for Re(CO)₅Cl. However, hydrosilylation with substrates such as 1,3-diketones, anthraquinones, and acetylacetonone did not occur even after extended photolysis of up to 12 h.

When the substrate was changed from acetone to benzaldehyde, an increase in the amount of product formed over the same period was observed (Table 1, entries 1 and 2). This can be attributed to the increased reactivity of aldehydes in comparison to that of ketones. When different silanes such as Ph₂SiH₂ and Ph₃SiH were used, a decrease in the corresponding silyl ether yield was observed (Table 2). The relatively lower rates toward hydrosilylation of acetone appear to bear a strong relation to the steric hindrance of the silane. In addition, when the carbonyl substrate was changed from aliphatic to a hindered aromatic carbonyl, i.e. benzophenone, acetophenone, and benzaldehyde, a decrease in the TOF was observed.

Hydrosilylation of Esters and Carbonates. In the presence of Re(CO)₅Cl, esters and carbonates have been reduced with silanes, although at a lower rate in comparison to that for the aldehydes. Under our experimental conditions, the reaction of ethyl acetate and Et₃SiH gave ethoxytriethylsilane as the main product with a trace amount of diethyl ether. Acetaldehyde has been detected as an intermediate whereby its signal intensity decreases upon further photolysis while that of ethoxytriethylsilane continues to increase (Figure 2). Similar results have been obtained for methyl phenylacetate and methyl formate.

Table 2. Reactions of Acetone and Benzaldehyde with Various Silanes (Silane:Carbonyl = 3:1)

Entry	Substrate	Silane	Time	Product	TON ^[a] (hr ⁻¹) ^[b]
1		Ph ₃ SiH	10hrs		1
2		Ph ₃ SiH	10hrs		1.5
3		Ph ₂ SiH ₂	5hrs		8
4		Ph ₂ SiH ₂	5hrs		10
5		Me ₂ PhSiH	5hrs		8
6		Me ₂ PhSiH	5hrs		14

^aTON calculated on the basis of 1% mol loading of Re(CO)₅Cl. The yield of the product was determined on the basis of the integration of the ¹H NMR spectra using toluene as standard.

The reaction of Et₃SiH with diethyl carbonate afforded a variety of products, with Et₃SiOEt (1) and EtOCH₂OSiEt₃ (2) being the major ones. A trace amount of ethyl formate, EtOCHO (3), has been detected. When the reaction mixture was left overnight, ¹H NMR peaks belonging to (EtO)₂CH₂ (4) were detected along with a decrease in 1 and 2.

Comparison of Hydrosilylation Rates for Different Carbonyls. By comparing the ratio of the products within the same photolysis period, the following general relationship has been determined for the relative rate using Re(CO)₅Cl and Et₃SiH: aliphatic aldehydes > aromatic aldehydes > aliphatic ketones > aromatic ketones ≈ esters (Table 3). On comparison within each functional group, the alkyl analogues are more reactive than their aryl counterparts. Using pyruvic acid which has both C=O and O–H groups, it was found that Et₃SiH

Table 3. Ratio of Hydrosilylation Products Formed^c

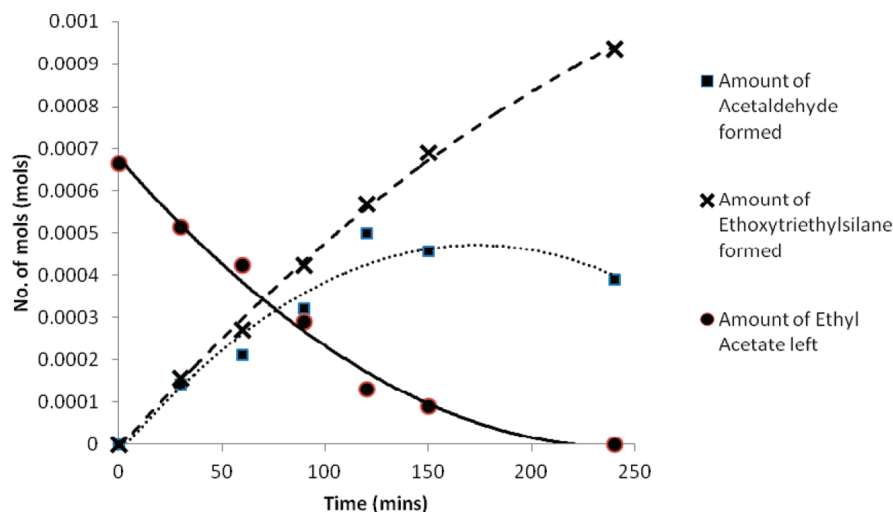
Entry	Substrate	Product	Ratio ^{[a],[b]}
1	Ethanal		90
2	Propanal		90
3	Benzaldehyde		9
4	Acetone		1
5	Acetophenone		0.5
6	Benzophenone		0.03
7	Ethyl Acetate		0.25
8	Pyruvic Acid		480

^aRatio with respect to acetone. ^bYield calculated on the basis of the integration of the ¹H NMR spectra using toluene as standard. ^cRelative rates were determined by adding 3:1:1 ratio of Et₃SiH with various carbonyl substrates and acetone.

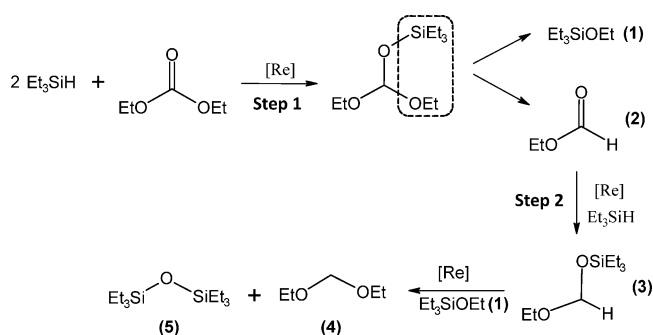
preferentially reacted with the O–H group to produce the silyl ester.

Mechanism. The identification of the organic intermediates and products suggests that the first step of hydrosilylation proceeds via addition of R₃SiH across the carbonyl group, except when an O–H group is present. The formation of both H₂ and a strong Si–O bond provides much of the driving force behind the reaction between the alcohol and silane. However, our focus is on the addition reaction; hence, the complex reaction pathways for the diethyl carbonate case are highlighted as an example (Scheme 2).

The products of the reaction between Et₃SiH and diethylcarbonate were observed and identified by ¹H NMR (Experimental Section) and were attributed to triethylethoxysilane (1), ethyl formate (2), ethoxymethoxytriethylsilane (3), diethoxymethane (4) and hexaethylsiloxane (5). The formation of these products led us to postulate the following mechanism.

**Figure 2.** ¹H NMR intermediate studies on the amount of intermediates and products produced during the reaction of ethyl acetate and Et₃SiH.

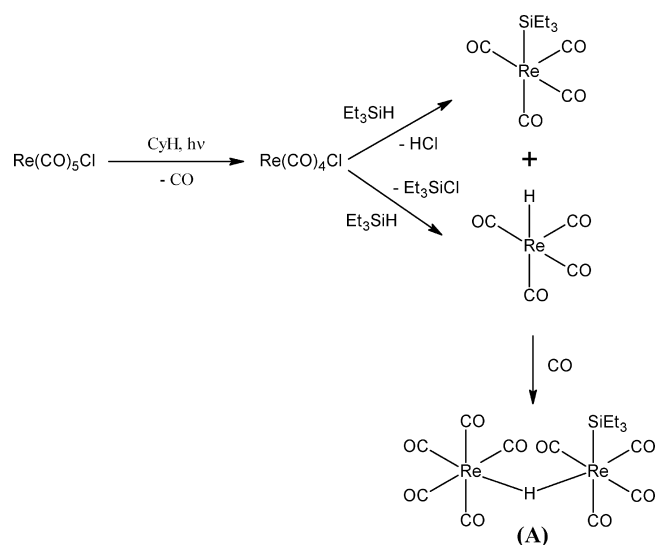
Scheme 2. Proposed Reaction Scheme of the Stepwise Reaction



An unstable silyl acetal intermediate is first formed, which undergoes “condensation” to afford **1** and **2**. With excess silane, ethyl formate (**2**) can be further reduced to **3**. This explains the relatively small amount of formate left in the mixture. In addition, the experimental data also suggested that compound **1** undergoes further reaction with **2** to generate the ether **4** and siloxane **5**.

As one of the main objectives of this work is to elucidate the mechanism of hydrosilylation, FTIR spectroscopy has been utilized for the detection of any metal carbonyl intermediates present in the catalytic mixture. Upon photolysis of Et_3SiH with $\text{Re}(\text{CO})_5\text{Cl}$, a dimeric rhenium carbonyl species with a bridging hydride (henceforth known as complex **A**) has been identified in the mixture (Figure 3). The identification of the complex was based on the IR spectral resemblance to rhenium complexes²¹ of formula $\text{HRe}_2(\text{CO})_9(\text{SiR}_3)$. Its bridging hydride signal at -9.03 ppm has also been recorded in the NMR spectrum. The diphenylsilyl analogue, complex **B**, has also been prepared upon $\text{Re}(\text{CO})_5\text{Cl}$ photolysis in the presence of diphenylsilane. Other than **A**, another hydride signal at -5.77 ppm found in the reaction mixture has been attributed to $\text{HRe}(\text{CO})_5$.

The formation of complex **A** can be rationalized as follows (Scheme 3). Upon UV photolysis of $\text{Re}(\text{CO})_5\text{Cl}$, a CO ligand dissociates to form the 16-electron $\text{Re}(\text{CO})_4\text{Cl}$ intermediate followed by Et_3SiH coordination. Upon reductive elimination, either HCl or Et_3SiCl is formed together with the corresponding $\text{Et}_3\text{SiRe}(\text{CO})_4$ or $\text{HRe}(\text{CO})_4$ species. A free CO molecule coordinates back to $\text{HRe}(\text{CO})_4$ to give $\text{HRe}(\text{CO})_5$. The bridging of its hydride ligand to $\text{Et}_3\text{SiRe}(\text{CO})_4$ would then result in the formation of **A**.

Scheme 3. Formation of **A** from $\text{Re}(\text{CO})_5\text{Cl}$ Photolysis in Et_3SiH 

When **A** was isolated and tested for aldehyde hydrosilylation, the silyl ether was generated about 2–3 times faster in comparison to $\text{Re}(\text{CO})_5\text{Cl}$. UV irradiation is still essential for the catalysis to occur. The IR signals of **A** persisted even after the end of catalysis, with a recovery of about 70–80%.

Interestingly, complex **A** can also be generated upon $\text{Re}_2(\text{CO})_{10}$ photolysis in triethylsilane, which would explain the similarity in the reaction rate to $\text{Re}(\text{CO})_5\text{Cl}$. From these observations, there are reasons to believe that complex **A** acts as a resting state in carbonyl hydrosilylation. One of the crucial steps in the catalysis involves the photocleavage of **A** to form $\text{HRe}(\text{CO})_5$ and the 16-electron rhenium carbonyl $\text{Et}_3\text{SiRe}(\text{CO})_4$. As it was shown earlier that catalysis with $\text{HRe}(\text{CO})_5$ is sluggish, we believe that the rhenium silyl species is most likely the active catalytic species instead.

A mechanism for the hydrosilylation of carbonyl compounds is proposed to account for the experimental observations (Scheme 4). Upon photolysis, **A** dissociates to afford $\text{Et}_3\text{SiRe}(\text{CO})_4$. Then the carbonyl substrate undergoes coordination onto the vacant site and facilitates the silyl ligand shift onto the oxygen atom. This process results in the formation of an alkyl ligand bound to the Re center (steps 1

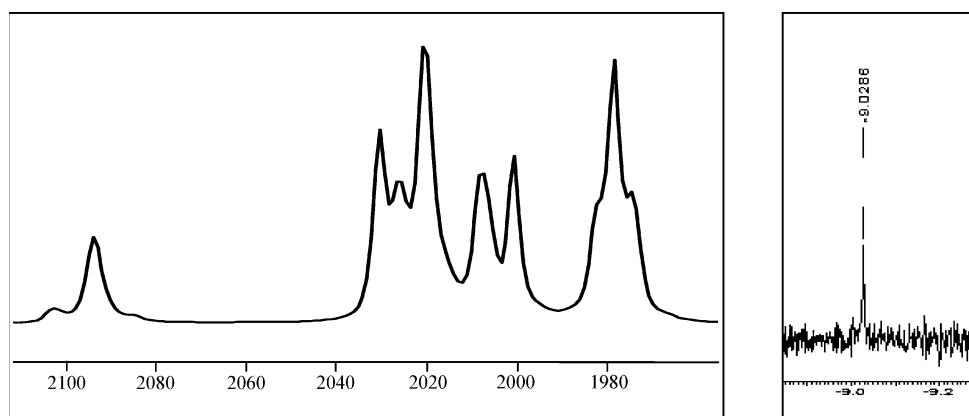
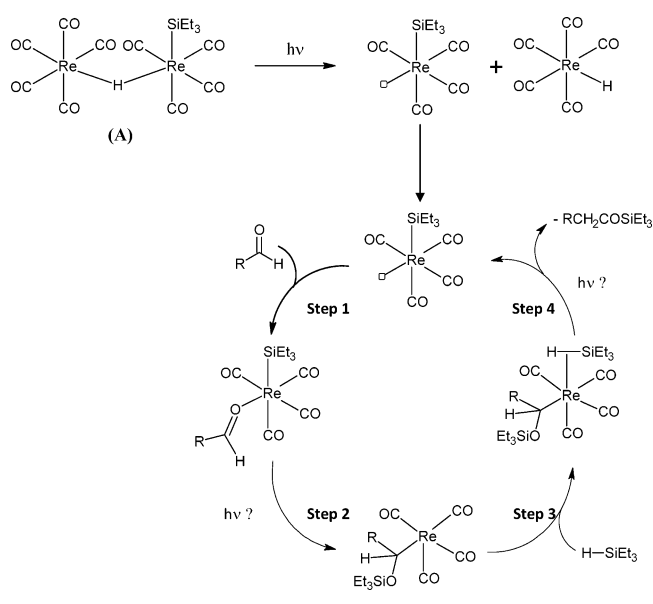


Figure 3. IR (left) and ^1H hydride NMR (right) spectra of **A** obtained from photolysis of $\text{Re}(\text{CO})_5\text{Cl}$ with Et_3SiH . IR (cm^{-1}): 2102, 2094, 2085, 2030, 2026, 2020, 2007, 2000, 1978; lit.¹³ for $\text{HRe}_2(\text{CO})_9\text{SiCl}_3$ 2150, 2095, 2085, 2047, 2019, 2012, 1999, 1978. ^1H NMR (ppm): -9.03 .

Scheme 4. Proposed Mechanism of the Hydrosilylation Reaction



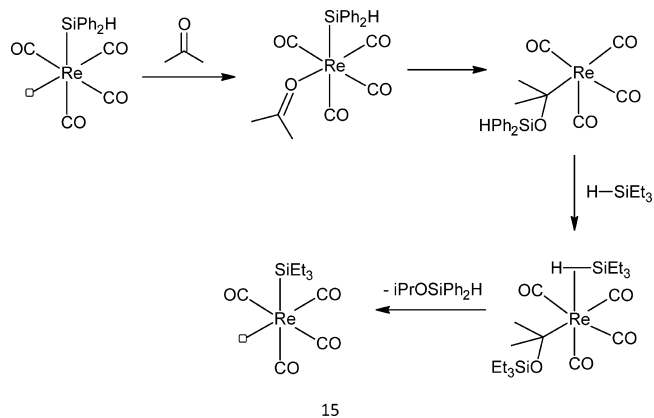
and 2). Another silane undergoes coordination via a η^2 -silyl complex^{4,7} or a σ -silyl (σ_{H}) complex (step 3). The H atom migrates from the silane to the alkyl group, thus regenerating the catalyst and releasing the silyl ether product (step 4). When either the carbonyl or silane has been depleted, the $\text{R}_3\text{SiRe}(\text{CO})_4$ coordinates back to $\text{HRe}(\text{CO})_5$ and becomes part of the resting state (A).

While the bond formation of steps 1 and 3 would proceed thermally, we are uncertain whether the catalytic cycle requires photons to initiate steps 2 and 4. A crude estimate of the quantum yield for the production of $\text{iPrO}(\text{SiEt}_3)$ was carried out by calibrating to the quantum yield (0.06 at 366 nm and 0.44 at 313 nm) for CO dissociation from $\text{Re}(\text{CO})_5\text{Cl}$. Since our broad-band irradiation covers both wavelengths, we have assumed an average quantum yield value of 0.25 for the experiments. By conducting the measurements during the first 1 h of catalysis, a quantum yield of 7.5 ± 4.8 has been determined using this method (see the Experimental Section). The value here suggests that the cycle proceeds without light. However, due to the large measurement error, further investigation into this catalytic cycle is required.

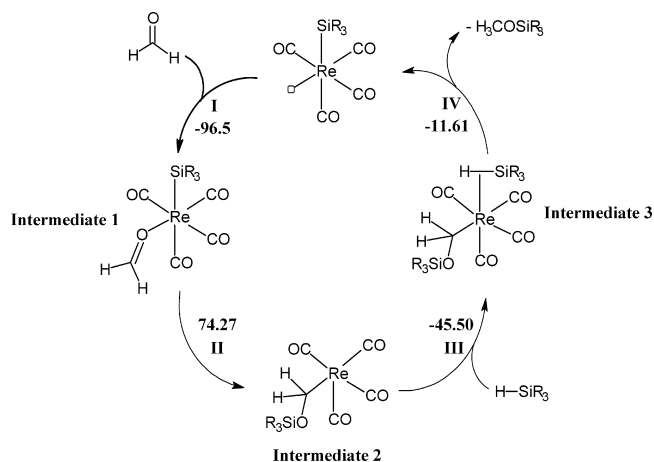
The activity of A in the catalytic cycle can be tested by using its Ph_2SiH_2 analogue, B, to catalyze the hydrosilylation of acetone and Et_3SiH . Upon completion of catalysis, ^1H NMR analysis showed the presence of $\text{iPrO}(\text{SiEt}_3)$ as the expected main product with a small amount of $\text{iPrO}(\text{SiHPh}_2)$. More importantly, the IR spectrum has changed from that of B to A. These observations show that silyl exchange has occurred between B and the free Et_3SiH during catalysis and lends support to A participating in the catalysis (Scheme 5).

Calculations. Computational studies have been carried out to show the thermodynamic feasibility of the catalytic cycle in Scheme 4 and to provide a general explanation for the relative rates of hydrosilylation among different carbonyl substrates. The energetics and structures of the complexes together with any transition states have been calculated using the mp2/lanl2dz level of theory and basis set in Gaussian 03.²² Vibrational frequencies were calculated for the optimized structures. In order to save computational time, formaldehyde

Scheme 5. Silane Exchange from B to A during the Reaction



(CH_2O) and silane (SiH_4) have been used as the substrates as shown in Scheme 6. Solvent effects have not been computed as well.

Scheme 6. Calculated Catalytic Cycle for SiH_4 and CH_2O^a 

^aValues quoted are for free energies in kJ/mol.

Table 4 shows the relevant thermodynamic parameters and ν_{CO} frequencies for the intermediates (restricted to singlet states only) and transition states found for the cycle, while the calculated structures of the relevant intermediates and transition states are found in Figure 4. The calculations showed that steps I and III in Scheme 6 are exoergic, due to coordination of substrates to the relevant rhenium complexes. In contrast, step II is endoergic, as activation is required for the silyl transfer to the carbonyl ligand in order to form intermediate II. The transition state TSI for this step has been found and optimized with an activation energy of 74.3 kJ/mol relative to intermediate I or 9.6 kJ/mol relative to CH_2O and $\text{Re}(\text{CO})_4\text{SiH}_3$. The reaction coordinate correctly depicts the migration of the silyl to the O atom of formaldehyde at an imaginary frequency of $281i \text{ cm}^{-1}$. Step IV turns out to be exoergic with a transition state TSII at only 26.0 kJ/mol relative to intermediate 3. The reaction coordinate for this transition state shows an almost linear migration of an H atom from silane to the alkyl group at an imaginary frequency of $798i \text{ cm}^{-1}$. The formation of the strong C–H bond is the driving force behind the reaction and accounts for the relatively lower activation barrier. By comparison of the energies, step II represents the

Table 4. Calculated Enthalpies (hartree), Free Energies (hartree), Carbonyl Vibrational and Imaginary Frequencies (cm^{-1}), and Activation Barriers to TS1 (kJ/mol, Relative to $\text{Re}(\text{CO})_4\text{SiH}_3$ and the Respective Carbonyl) for the Rhenium Intermediates and Transition States of the Catalytic Cycle^a

complex	enthalpy H	free energy G	ν_{CO} or i	E_a
Structures for CH_2O Substrate				
$\text{H}_3\text{SiRe}(\text{CO})_4$	-535.751 262	-535.806 047	1767, 1807, 1809, 1908	
intermediate I	-649.819 307	-649.880 743	1775, 1784, 1818, 1908	
intermediate II	-649.791 523	-649.852 45	1779, 1792, 1820, 1916	
intermediate III	-655.891 354	-655.960 371	1767, 1784, 1808, 1921	
TSI	-649.783 078	-649.840 337	1789, 1799, 1817, 1900, 281i	9.6
TSII	-655.882 012	-655.950 457	1797, 1820, 1832, 1921, 798i	
Transition States for Different Substrates				
TSI for HCOOCH_3	-763.804 788	-763.868 593	1781, 1793, 1821, 1907, 291i	67.7
TSI for $(\text{CH}_3)_2\text{CO}$	-727.961 207	-728.024 76	1777, 1793, 1805, 1900, 279i	24.0
TSI for PhCHO	-879.689 834	-879.758 904	1780, 1792, 1809, 1902, 265i	2.0

^aThe silane used is SiH_4 , and the method and basis set used is mp2/lanl2dz.

rate-determining step in the catalytic cycle. The activation barrier of 74.3 kJ/mol for step II together with the time needed to generate sufficient $\text{Re}(\text{CO})_4\text{SiR}_3$ could perhaps account for the period of several hours required for the completion of catalysis at 300 K.

The relative hydrosilylation rates can be explained by comparing the activation barriers of the rate-determining step for the different substrates. We have focused on optimizing the respective transition states **TS 1** of four representative carbonyls: formaldehyde, benzaldehyde, acetone, and methyl formate. The value of the activation barrier is calculated relative to the starting pair in the cycle: i.e., $\text{Re}(\text{CO})_4\text{SiH}_3$ and the corresponding carbonyl. The various transition states together with the essential molecular parameters have been depicted in Figure 5. On comparison of the values of E_a in Table 4, it can be seen that the barriers for the aldehydes are lower than that for the ketone, which itself is much lower than that for the ester. In the ester case, electronic effects due to the OR group destabilize the transition state much more than the aldehyde or ketone counterpart. Interestingly, the calculated activation energy for the benzaldehyde system is the lowest, despite experimental kinetic studies suggesting a faster reaction for aliphatic aldehydes. Although the difference is slight (~ 7 kJ/mol), the inclusion of solvent effects may be able to reverse this trend.

CONCLUSION

$\text{Re}(\text{CO})_5\text{Cl}$ has been found to catalyze the hydrosilylation reaction between various silanes and carbonyl substrates such as aldehyde, ketone, ester, and carbonate effectively with a turnover frequency of 20–25 h^{-1} for aldehydes. The rates of hydrosilylation are highest for the least sterically hindered silanes with aldehydes, followed by aliphatic ketone. Aromatic ketone, ester, and carbonate react most slowly with the silanes. The rhenium dimer complex $\text{HRe}_2(\text{CO})_9$, has been detected using

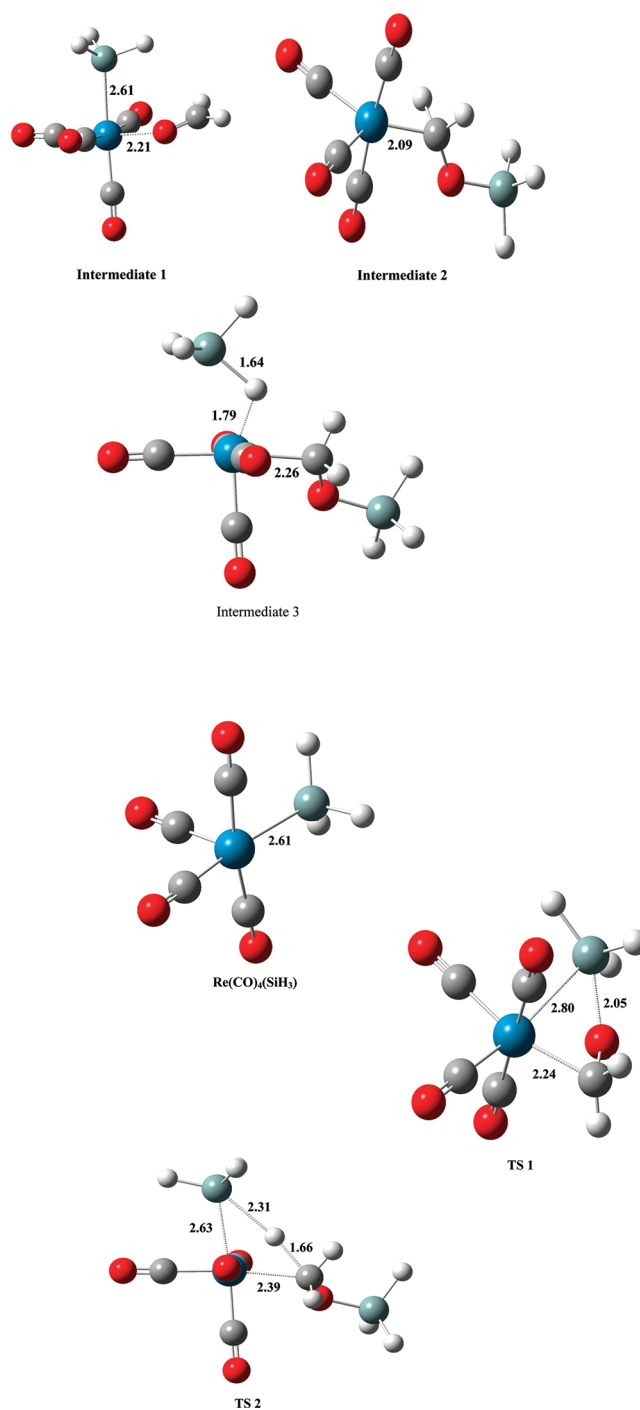


Figure 4. Calculated structures of intermediates and transition states for Scheme 6. Essential bond lengths (Å) are shown.

IR spectroscopy and is believed to be the resting state for the catalysis. Upon its photolysis, the active catalyst $\text{Re}(\text{CO})_4\text{SiH}_3$ is released and participates in the catalytic cycle. Computational studies have shown that the proposed cycle can be carried out readily at room temperature and are able to explain the relative hydrosilylation rates among the various carbonyl substrates.

EXPERIMENTAL SECTION

All chemicals were used as purchased. All reactions were carried out under vacuum conditions unless otherwise stated. Proton nuclear magnetic resonance (^1H NMR) spectra were obtained on a Bruker Avance 500 (AV500) spectrometer at room temperature. The

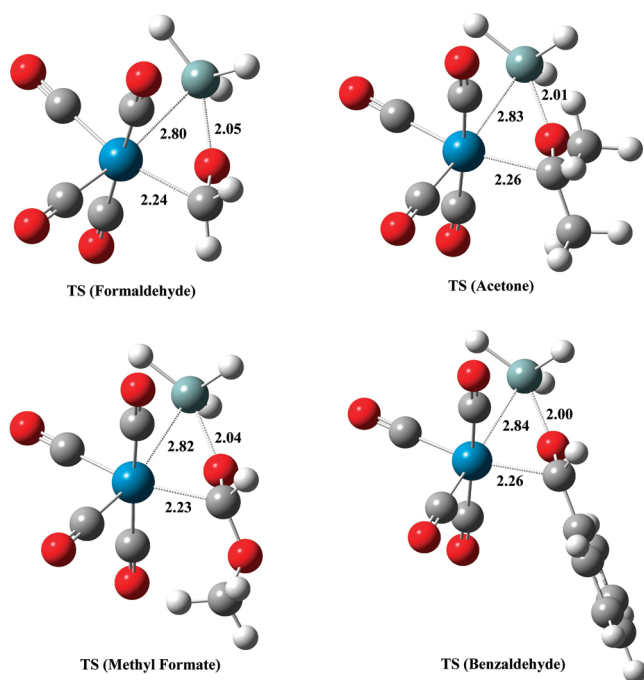


Figure 5. Optimized transition states for the rate-determining steps of different substrates. Bond lengths are given in Å.

chemical shifts were recorded relative to tetramethylsilane for spectra taken in CDCl_3 .

Infrared (IR) spectra were obtained on a Shimadzu IR Prestige-21 Fourier-transform infrared spectrometer ($1000\text{--}4000\text{ cm}^{-1}$, 1 cm^{-1} resolution, 4 scans coadded for spectra averaging) using a 0.05 mm path length CaF_2 cell. Mass spectra of the organic products were recorded with a Finnigan Mat 95XL-T spectrometer.

Catalysis using $\text{Re}(\text{CO})_5\text{Cl}$. $\text{Re}(\text{CO})_5\text{Cl}$ (0.011 mmol) was mixed with Et_3SiH (3.3 mmol) and the carbonyl substrate (1.1 mmol) in a quartz tube. The mixture was photolyzed in vacuo, using a Legrand broad-band lamp (200–800 nm, 11 W) for 4 h. Products were identified using $^1\text{H NMR}$. For one control experiment, PPh_3 (0.03 mmol) was added to the reaction mixture as described above.

Catalytic Reduction of Diethyl Carbonate. $\text{Re}(\text{CO})_5\text{Cl}$ (0.011 mmol) was mixed with Et_3SiH (3.3 mmol) and diethyl carbonate (1.1 mmol) in a quartz tube. The mixture was photolyzed in vacuo, using a Legrand broad-band lamp (200–800 nm, 11 W) for 4 h. $^1\text{H NMR}$ (CDCl_3 , ppm): triethylethoxysilane (1), 0.60 (m), 0.98 (m), 1.20 (m), 3.65 (m); ethyl formate (2), 1.31 (t), 4.24 (q), 8.04 (s); diethoxymethane (4), 0.60 (m), 0.98 (m), 1.20 (m), 3.65 (m), 4.86 (m).

Synthesis of $\text{HRe}(\text{CO})_5$. $\text{HRe}(\text{CO})_5$ was synthesized via a modification of reported methods.^{23–25} A 0.011 mmol amount of $\text{Re}(\text{CO})_5\text{Cl}$ was dissolved in methanol, and the mixture was stirred for 1 h, after which the mixture was cooled using liquid nitrogen. Excess zinc and acetic acid were then added to the cooled mixture before evacuation of the air inside the round-bottom flask was done. The reaction mixture was then stirred for 24 h at room temperature. The $\text{HRe}(\text{CO})_5$ formed was extracted using $3 \times 3\text{ mL}$ of hexane and recrystallized using CHCl_3 . ν_{CO} (cyclohexane, cm^{-1}): 2015 (vs), 2005 (m), 1983 (w). $^1\text{H NMR}$: -5.77 ppm .

Comparison of Rate of Hydroxylation Reaction between Different Substrates. $\text{Re}(\text{CO})_5\text{Cl}$ (0.011 mmol) was mixed with Et_3SiH (3.3 mmol) and two different carbonyl substrates (1.1 mmol each) in a quartz tube. The mixture was photolyzed in vacuo, using a Legrand broad-band lamp (200–800 nm, 11 W) for 4 h. Products were identified using $^1\text{H NMR}$, and yields were calculated with toluene (0.011 mmol) as standard.

Synthesis of $\text{HRe}_2(\text{CO})_9(\text{SiR}_3)$ from $\text{Re}(\text{CO})_5\text{Cl}$. $\text{Re}(\text{CO})_5\text{Cl}$ (0.011 mmol) and R_3SiH (0.022 mmol) were dissolved in cyclohexane

in a quartz tube. The mixture was photolyzed in vacuo, using a Legrand broad-band lamp (200–800 nm, 11 W) until all ν_{CO} bands of $\text{Re}(\text{CO})_5\text{Cl}$ disappeared (2–4 h). The yellow solution was concentrated and passed through a column using a 1:1 mixture of hexane and chloroform. The resultant yellow band was then collected and the solvent removed using vacuum and recrystallized in hexane solution to afford a yellow powder (the yield with respect to $\text{Re}(\text{CO})_5\text{Cl}$ is 65%). The products were identified on the basis of a comparison of their IR and $^1\text{H NMR}$ spectra to reported values.¹⁵

$\text{HRe}_2(\text{CO})_9(\text{SiEt}_3)$: ν_{CO} (cyclohexane, cm^{-1}) 2030 (m), 2021 (s), 2016 (sh), 2008 (m), 2000 (m), 1982 (sh), 1978 (s); $^1\text{H NMR}$ (ppm) -9.03 ; UV (nm) 200–400 (broad with λ_{max} 218 nm); ESI mass spectrum (m/e) 742.

$\text{HRe}_2(\text{CO})_9(\text{SiPh}_2\text{H})$: ν_{CO} (cyclohexane, cm^{-1}) 2029 (m), 2020 (s), 2014 (sh), 2008 (m), 2000 (m), 1981 (sh), 1976 (s); $^1\text{H NMR}$ (ppm) -9.71 .

Synthesis of $\text{HRe}_2(\text{CO})_9(\text{SiEt}_3)$ from $\text{Re}_2(\text{CO})_{10}$. $\text{Re}_2(\text{CO})_{10}$ (0.011 mmol) and Et_3SiH (0.022 mmol) were dissolved in cyclohexane in a quartz tube. The mixture was photolyzed in vacuo, using a Legrand broad-band lamp (200–800 nm, 11 W) until all ν_{CO} bands of $\text{Re}(\text{CO})_5\text{Cl}$ disappeared (2–4 h). The yellow solution was concentrated and passed through a column using a 1:1 mixture of hexane and chloroform. The resultant yellow band was then collected and the solvent removed using vacuum and recrystallized in hexane solution to afford a yellow powder (the yield with respect to $\text{Re}(\text{CO})_5\text{Cl}$ is 68%).

Quantum Yield Estimation for $\text{Re}(\text{CO})_5\text{Cl}$ Catalysis of Et_3SiH and Acetone. $\text{Re}(\text{CO})_5\text{Cl}$ (0.011 mmol) was added to cyclohexane (3 mL) in a quartz tube. The mixture was subjected to freeze–pump–thaw three times before it was broad band irradiated for 1 h. The dissociated amount of $\text{Re}(\text{CO})_5\text{Cl}$ ($=[\text{Re}(\text{CO})_5\text{Cl}]_{t=0} - [\text{Re}(\text{CO})_5\text{Cl}]_{t=1\text{ h}}$) was noted as x . The concentrations of the complexes were derived from Beer's law via the IR absorbance. $\text{Re}(\text{CO})_5\text{Cl}$ (0.011 mmol), acetone (1.1 mmol), and Et_3SiH (1.1 mmol) were added to cyclohexane (3 mL) in a quartz tube. The mixture was subjected to freeze–pump–thaw three times before it was broad band irradiated for 1 h. The concentration of the $\text{iPrO}(\text{SiEt}_3)$ product (from $^1\text{H NMR}$ analysis) was noted as y . This series of reactions was repeated four times.

The estimate of the quantum yield for the catalysis is $(y/x) \times 0.25$. The value of 0.25 represents an “average” quantum yield of $\text{Re}(\text{CO})_5\text{Cl}$ dissociation from 300 to 400 nm.¹⁹ The x value is proportional to this quantum yield of 0.25. Under the described experimental conditions above, $y = 0.12 \pm 0.05\text{ mmol}$ and $x = 0.004 \pm 0.002\text{ mmol}$, and hence the quantum yield for catalysis is 7.5 ± 4.8 .

Silyl Exchange between $\text{HPh}_2\text{SiRe}(\text{CO})_4$ and Et_3SiH . Et_3SiH (0.22 mmol) and acetone (0.11 mmol) were added to a cyclohexane solution containing $\text{HRe}_2(\text{CO})_9(\text{SiR}_3)$ (0.011 mmol) in a quartz tube. The mixture was photolyzed in vacuo, and an IR spectrum of the reaction was taken at every 30 min interval.

AUTHOR INFORMATION

Corresponding Author

*Correspondence: chmfanwy@nus.edu.sg.

Notes

The authors declare no competing financial interest.

ACKNOWLEDGMENTS

The project was supported by a research grant provided by NUS 143-000-430-112. C.K.T. acknowledges the support of a NUS scholarship.

REFERENCES

- (1) Abu-Omar, M. M.; Du, G. *Organometallics* **2006**, *25*, 4920–4923.
- (2) Morris, R. H. *Chem. Soc. Rev.* **2009**, *38*, 2282–2291.
- (3) Shaikh, N. S.; Junge, K.; Beller, M. *Org. Lett.* **2007**, *9*, 5429–5432.
- (4) Fernandes, A. C.; Fernandes, R.; Romão, C. C.; Royo, B. *Chem. Commun.* **2005**, 213–214.

- (5) Gądek, A.; Szymańska-Buzar, T. *Polyhedron* **2006**, *25*, 1441–1448.
- (6) Son, S. U.; Paik, S.; Chung, Y. K. *J. Mol. Catal. A: Chem.* **2000**, *151*, 87–90.
- (7) Cavanaugh, M. D.; Gregg, B. T.; Cutler, A. R. *Organometallics* **1996**, *15*, 2764–2769.
- (8) Dong, H.; Berke, H. *Adv. Synth. Catal.* **2009**, *351*, 1783–1788.
- (9) Ojima, I.; Nihonyanagi, M.; Kogure, T.; Kumagai, M.; Horiuchi, S.; Nakatsugawa, K. *J. Organomet. Chem.* **1975**, *94*, 449–461.
- (10) Wile, B. M.; Stradiotto, M. *Chem. Commun.* **2006**, 4104–4106.
- (11) Do, Y.; Han, J.; Rhee, Y. H.; Park, J. *Adv. Synth. Catal.* **2011**, *353*, 3363–3366.
- (12) Chung, L. W.; Lee, H. G.; Lin, Z.; Wu, Y. J. *Org. Chem.* **2006**, *71*, 6000–6009.
- (13) Du, G.; Fanwick, P. E.; Abu-Omar, M. M. *J. Am. Chem. Soc.* **2007**, *129*, 5180–5187.
- (14) Sharma, H. K.; Pannell, K. H. *Angew. Chem., Int. Ed.* **2009**, *48*, 7052–7054.
- (15) Mao, Z.; Gregg, B. T.; Cutler, A. R. *J. Am. Chem. Soc.* **1995**, *117*, 10139–10140.
- (16) Ojima, Y.; Yamaguchi, K.; Mizuno, N. *Adv. Synth. Catal.* **2009**, *351*, 1405–1411.
- (17) Gevorgyan, V.; Rubin, M.; Liu, J.; Yamamoto, Y. *J. Org. Chem.* **2001**, *66*, 1672–1675.
- (18) Hua, R.; Jiang, J. *Curr. Org. Synth.* **2007**, *4*, 151–174.
- (19) Wrighton, M. S.; Morse, D. L.; Gray, H. B.; Ottessen, D. K. *J. Am. Chem. Soc.* **1976**, *98*, 1111–1119.
- (20) Zingales, F.; Sartorelli, U.; Canziani, F.; Raveglia, M. *Inorg. Chem.* **1967**, *6*, 154–157.
- (21) Hoyano, J. K.; Graham, W. A. G. *Inorg. Chem.* **1972**, *11*, 1265–1269.
- (22) Frisch, M. J.; et al. *Gaussian 03, Revisions B and B.05*; Gaussian Inc., Wallingford, CT, 2004.
- (23) Braterman, P. S.; Harrill, R. W.; Kaesz, H. D. *J. Am. Chem. Soc.* **1967**, *89*, 2851–2855.
- (24) Byers, B. H.; Brown, T. L. *J. Am. Chem. Soc.* **1977**, *99*, 2527–2532.
- (25) Li, N.; Xie, Y.; King, R. B.; Schaefer, H. F., III *J. Phys. Chem. A* **2010**, *114*, 11670–11680.